Multiplexing of polarization-maintaining photonic crystal fiber based Sagnac interferometric sensors

H. Y. Fu,[1] A. C. L. Wong,[2] P. A. Childs,[3] H. Y. Tam,[1†] Y. B. Liao,[3] C. Lu,[2] and P. K. A. Wai[2]

[1]*Photonics Research Centre, Department of Electrical Engineering, The Hong Kong Polytechnic University, Hung Hom, Kowloon, Hong Kong SAR, China*

[2]*Photonics Research Centre, Department of Electronic and Information Engineering, The Hong Kong Polytechnic University, Hung Hom, Kowloon, Hong Kong SAR, China*

[3]*Department of Electronic Engineering, Tsinghua University, Beijing 100084, China*

[†] *eehytam@polyu.edu.hk*

Abstract: Three multiplexing schemes are presented for polarization-maintaining photonic crystal fiber based Sagnac interferometric sensors. The first technique is wavelength division multiplexing using coarse wavelength division multiplexers (CWDMs) to distinguish signals from each multiplexed sensor in different wavelength channels. The other two schemes are to multiplex sensors in series along a single fiber link and in parallel by using fiber-optic couplers. While for the CWDM scheme, the multiplexed sensing signal can be obtained by direct measurement; for the other two multiplexing techniques, the sensing signal is more complex and cannot be easily demultiplexed. Thus, some signal processing methods are required. In this regard, two mathematical transformations, namely the discrete wavelet transform and Fourier transform, have been independently and successfully implemented into these two schemes. The operating principles, experimental setup, and overall performance are discussed.

OCIS codes: (060.2370) Fiber optics sensors; (060.4230) Multiplexing; (060.5295) Photonic crystal fibers; (120.5790) Sagnac effect; (060.2420) Fibers, polarization-maintaining.

References and links

1. J. C. Knight, T. A. Birks, P. St. J. Russell, and D. M. Atkin, "All-silica single-mode optical fiber with photonic crystal cladding," Opt. Lett. **21**(19), 1547–1549 (1996).
2. T. A. Birks, J. C. Knight, and P. S. Russell, "Endlessly single-mode photonic crystal fiber," Opt. Lett. **22**(13), 961–963 (1997).
3. P. St. J. Russell, "Photonic crystal fibers," Science **299**(5605), 358–362 (2003).
4. T. M. Monro, W. Belardi, K. Furusawa, J. C. Baggett, N. G. R. Broderick, and D. J. Richardson, "Sensing with microstructured optical fibres," Meas. Sci. Technol. **12**(7), 854–858 (2001).
5. B. J. Eggleton, C. Kerbage, P. S. Westbrook, R. S. Windeler, and A. Hale, "Microstructured optical fiber devices," Opt. Express **9**(13), 698–713 (2001), http://www.opticsinfobase.org/oe/abstract.cfm?URI=OPEX-9-13-698.
6. O. Frazão, J. L. Santos, F. M. Araujo, and L. A. Ferreira, "Optical sensing with photonic crystal fibers," Laser Photon. Rev. **2**(6), 449–459 (2008).
7. C.-L. Zhao, X. Yang, C. Lu, W. Jin, and M. S. Demokan, "Temperature-insensitive interferometer using a highly birefringent photonic crystal fiber loop mirror," IEEE Photon. Technol. Lett. **16**(11), 2535–2537 (2004).
8. D.-H. Kim, and J. U. Kang, "Sagnac loop interferometer based on polarization maintaining photonic crystal fiber with reduced temperature sensitivity," Opt. Express **12**(19), 4490–4495 (2004), http://www.opticsinfobase.org/abstract.cfm?URI=oe-12-19-4490.
9. X. Y. Dong, H. Y. Tam, and P. Shum, "Temperature-insensitive strain sensor with polarization-maintaining photonic crystal fiber based Sagnac interferometer," Appl. Phys. Lett. **90**(15), 151113–3 (2007).
10. O. Frazao, J. M. Baptista, and J. L. Santos, "Temperature-independent strain sensor based on a Hi-Bi photonic crystal fiber loop mirror," IEEE Sens. J. **7**(10), 1453–1455 (2007).
11. H. Y. Fu, H. Y. Tam, L. Y. Shao, X. Dong, P. K. Wai, C. Lu, and S. K. Khijwania, "Pressure sensor realized with polarization-maintaining photonic crystal fiber-based Sagnac interferometer," Appl. Opt. **47**(15), 2835–2839 (2008).

#115518 - $15.00 USD Received 10 Aug 2009; revised 20 Sep 2009; accepted 21 Sep 2009; published 29 Sep 2009

12. O. Frazão, J. M. Baptista, J. L. Santos, and P. Roy, "Curvature sensor using a highly birefringent photonic crystal fiber with two asymmetric hole regions in a Sagnac interferometer," Appl. Opt. **47**(13), 2520–2523 (2008).
13. G. Kim, T. Cho, K. Hwang, K. Lee, K. S. Lee, Y.-G. Han, and S. B. Lee, "Strain and temperature sensitivities of an elliptical hollow-core photonic bandgap fiber based on Sagnac interferometer," Opt. Express **17**(4), 2481–2486 (2009), http://www.opticsinfobase.org/oe/abstract.cfm?uri=oe-17-4-2481.
14. M. L. V. Tse, H. Y. Tam, L. B. Fu, B. K. Thomas, L. Dong, C. Lu, and P. K. A. Wai, "Fusion splicing holey fibers and single-mode fibers: A simple method to reduce loss and increase strength," IEEE Photon. Technol. Lett. **21**(3), 164–166 (2009).
15. D. B. Mortimore, "Fiber Loop Reflectors," J. Lightwave Technol. **6**(7), 1217–1224 (1988).
16. L. Liu, Q. Zhao, G. Zhou, H. Zhang, S. Chen, L. Zhao, Y. Yao, P. Guo, and X. Dong, "Study on an optical filter constituted by concatenated Hi-Bi fiber loop mirrors," Microw. Opt. Technol. Lett. **43**(1), 23–26 (2004).
17. O. Frazao, J. L. Santos, and J. M. Baptista, "Strain and temperature discrimination using concatenated high-birefringence fiber loop mirrors," IEEE Photon. Technol. Lett. **19**(16), 1260–1262 (2007).
18. A. C. L. Wong, P. A. Childs, and G. D. Peng, "Multiplexed fibre Fizeau interferometer and fibre Bragg grating sensor system for simultaneous measurement of quasi-static strain and temperature using discrete wavelet transform," Meas. Sci. Technol. **17**(2), 384–392 (2006).
19. P. A. Childs, "An FBG sensing system utilizing both WDM and a novel harmonic division scheme," J. Lightwave Technol. **23**, 348–354 (2005), "Erratum" 23, 931 (2005).

1. Introduction

Photonic crystal fibers (PCFs), also known as microstructured optical fibers, are a new class of optical fiber that has generated a lot of research interest in recent years [1–3]. The flexibility in the design of PCFs distinguishes them from conventional fibers, and various PCFs have been developed targeting for different applications such as fiber-optic based sensing [4–6]. Polarization-maintaining PCFs (PM-PCFs), which have become commercially available, are one of these PCFs with the characteristics of having high birefringence and low temperature sensitivity. PM-PCFs implemented in Sagnac loops for sensing applications have been proposed and experimentally demonstrated as single sensors [7–13]. The multiplexing capability of Sagnac interferometric sensors thus plays a very important role if the sensors are to be expanded. Multiplexing can reduce the complexity of a sensor system, as well as the cost per sensing point by sharing the same optical source, interrogator and other components within the system. In addition, multi-parameter detection can be achieved within the same sensor system. However, at present, all of the published reports on any PCF-based sensing (not limited to only PM-PCFs) are operated as single sensors. There are two main reasons. The first is the high insertion loss at each splice/connection point, which reduces the signal-to-noise ratio of the sensing signals. In certain multiplexing schemes, splicing or connection with other fiber-optic components is individually required for each sensor. Additionally, splicing between PCFs and conventional single-mode fibers (SMFs) is required in order for PCF sensors to work with most common bench-top equipment and tools. The second reason is the difficulty in demultiplexing and demodulating the multiplexed PCF sensing signals. Even though the multiplexing schemes are simple and easy to implement, the multiplexed sensing signals can be quite complex, and so they cannot be demultiplexed easily. The first issue can be improved by employing low loss splicing techniques, such as the one we developed recently [14]. The second issue is the focus of this paper.

In this paper, three multiplexing schemes for PM-PCF based Sagnac interferometric sensors are presented. The first scheme is to multiplex sensors in the wavelength domain using coarse wavelength division multiplexers (CWDMs). The sensing signal from each sensor can be measured within a specific wavelength channel of the CWDM. The second scheme is to multiplex sensors by connecting them in series along a single fiber. It is simple in terms of system architecture as no additional fiber-optic components are needed. The third scheme is to multiplex sensors in parallel by using fiber-optic couplers. The sensing information of the first multiplexing technique can be obtained by direct measurement such as with an optical spectrum analyzer. For the serial and parallel multiplexing, signal processing methods are required to demultiplex the complex sensing signal. Two mathematical transformations, namely the discrete wavelet transform (DWT) and the Fourier transform (FT), are used independently to convert the multiplexed sensing signal back to their constituent sensor signals. These two transform methods are experimentally demonstrated via

#115518 - $15.00 USD Received 10 Aug 2009; revised 20 Sep 2009; accepted 21 Sep 2009; published 29 Sep 2009

two multiplexed Sagnac interferometric sensors. Their operating principles, experimental setup, and overall performance are discussed.

2. Principle of PM-PCF based Sagnac interferometric sensor

A brief review on the operating principle of Sagnac interferometric sensors is given in this section [15]. As illustrated in Fig. 1, it consists of a 3-dB fiber-optic coupler and a piece of PM-PCF (PM-1550-01, Blaze-Photonics®). The inset shows a scanning electron micrograph (SEM) of the cross-section of the PM-PCF. The PM-PCF is connected to the two ports on one side of the coupler. By using the low loss splicing technique [14], the total splicing loss between the PM-PCF and SMF was less than 4 dB with a good mechanical strength in all our experiments. Light from the source is split equally by the coupler into two beams which propagate in clockwise and counterclockwise directions. When passing through the coupler, the cross-coupled beam experienced a π/2 phase lag with respect to the direct beam traveling straight through the coupler. After experiencing different optical paths due to the birefringence of the PM-PCF, the two beams were fed back to the coupler and caused interference to occur. When illuminated with a broadband light source, the typical output spectrum of a Sagnac interferometer is a periodic sinusoidal pattern in the wavelength domain, which can be measured by an optical spectrum analyzer (OSA). The transmission matrix T of Sagnac interferometer can thus be written as,

$$T = \frac{1}{2}[1-\cos(\delta)]. \tag{1}$$

The phase difference δ introduced by the PM-PCF with a length of L to the two light beams is wavelength dependent and is given by,

$$\delta = \frac{2\pi BL}{\lambda}. \tag{2}$$

The period of the output spectrum, that is, the spacing between two adjacent minima, is $S=\lambda^2/(BL)$, where B is the birefringence of the PM-PCF. The birefringence change due to environmental parameters can then be detected by measuring the shift of transmission minima with an OSA. Earlier, we have reported the utilization of PM-PCF based Sagnac interferometers for pressure sensing [11]. Similar pressure sensing experiments were performed here for the purposes of demonstration and verification of the multiplexing schemes as well as the demultiplexing methods. The Sagnac interferometric sensors had a measured wavelength-pressure sensitivity coefficient of 0.34 nm/bar.

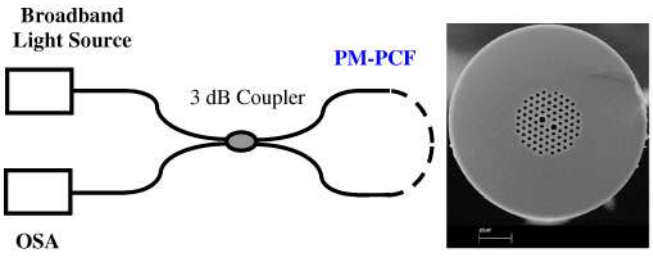

Fig. 1. Schematic of a PM-PCF based Sagnac interferometric sensor (PM-PCF indicated with dot line, the inset shows the SEM-image).

3. Multiplexing technique base on CWDM

Wavelength division multiplexing is a direct multiplexing technique that can be readily implemented into Sagnac interferometric sensors. Since the output interference spectra of all the sensors cover the whole bandwidth of the light source, individual sensor signals can be physically separated by CWDMs into different wavelength channels. The experimental setup of two multiplexed sensors using CWDMs is illustrated in Fig. 2. It includes a broadband light source, an OSA, two identical filter wavelength division multiplexers (FWDMs) with

#115518 - $15.00 USD Received 10 Aug 2009; revised 20 Sep 2009; accepted 21 Sep 2009; published 29 Sep 2009

the two output ports having respective operation range in the C and L bands (1500 ~1562 nm / 1570 ~1640 nm). The insertion loss was less than 0.4 dB and with a flatness of less than 0.3 dB. The two Sagnac interferometric sensors, PM-PCF1 and PM-PCF2, have effective PM-PCF lengths of 40 cm and 80 cm, respectively. After the broadband light was launched into the first FWDM, the light was split into C and L bands. These two bands of light then illuminated the two sensors separately and were recombined by the second FWDM. The OSA was used to measure the output spectrum.

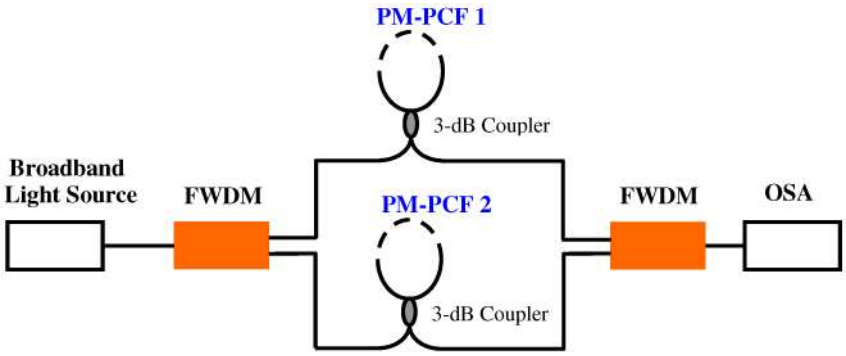

Fig. 2. Experimental setup of FWDM multiplexing technique for two PM-PCF based Sagnac interferometric sensors.

Figure 3 shows the output spectrum of the two Sagnac interferometric sensors multiplexed by FWDM. From the figure, sensors PM-PCF 1 and PM-PCF 2 are found in the L band and C band, respectively. The FWDMs are shown to have good flatness in their operating wavelength range. There is an abrupt discontinuity at the edges of the two FWDMs at around 1562 nm – 1570 nm, where such range should be excluded from measurements. By measuring the shifts of individual transmission minima (or maxima) of the two Sagnac interferometric sensors within their corresponding wavelength ranges, sensing information of both sensors can be obtained.

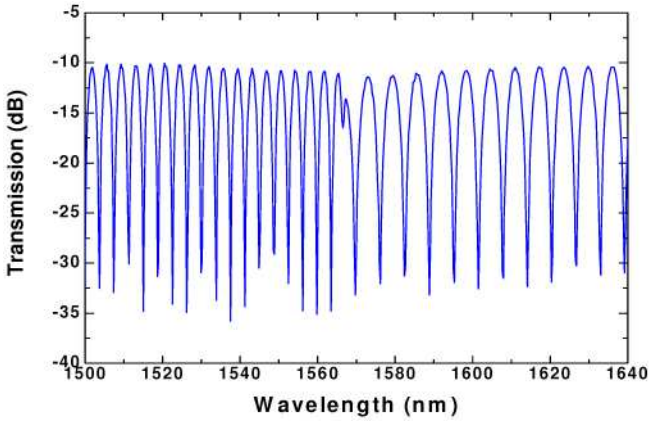

Fig. 3. Output Spectrum of the CWDM multiplexing technique for PM-PCF based Sagnac interferometric sensor.

4. Multiplexed in series along a single fiber with transmitted signals

The second multiplexing scheme is to multiplex Sagnac interferometric sensors in series along a single fiber. Similar concatenated sensor configuration has been employed previously in optical filtering [16], and in strain and temperature discrimination [17]. However, in both cases, multiplexing was not the main focus, and so the techniques of multiplexing were not

#115518 - $15.00 USD Received 10 Aug 2009; revised 20 Sep 2009; accepted 21 Sep 2009; published 29 Sep 2009

studied. Figure 4 illustrates such a scheme by simply cascading the sensors together. For K Sagnac interferometric sensors multiplexed in series, the output spectrum is given by,

$$\frac{P_{output}}{P_{input}} = 10Log_{10}\prod_{k=1}^{K}\left(\frac{1}{2}L_k\left[1-\cos(\frac{2\pi}{S_k}\lambda+\theta_k)\right]\right)[\mathrm{dB}], \quad (3)$$

where L_k, S_k, θ_k are the loss, the period of the output spectrum and the initial phase of the k-th sensor, respectively. Note that the output spectrum is the multiplication of all individual sensor signals.

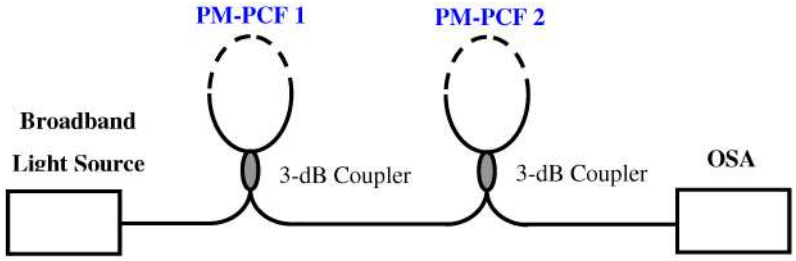

Fig. 4. Experimental setup of in series multiplexing technique for PM-PCF based Sagnac interferometric sensor.

In our experimental demonstration, two sensors were spliced together adjacent to each other in series. The effective lengths of PM-PCF1 and PM-PCF2 were 20 cm and 60 cm, respectively. PM-PCF1 was placed freely on a table, while PM-PCF2 was placed inside a sealed pressure chamber. Pressure was applied to PM-PCF2 from 0 – 3 bars in steps of 0.5 bar, and was measured by a pressure gauge (COMARK C9557). Figure 5 shows the output spectra of various pressure values measured by the OSA. In principle, to obtain the sensing information, the wavelength shift of the transmission minima of each sensor needs to be determined. However, as can be seen, the multiplexed sensor signal is more complex, and so simply tracing the initial phase may not yield accurate results. Thus, in order to separate the multiplexed signals, the DWT and FT methods were used independently to demultiplex the sensing signals. They worked by transforming the signals into another domain, such that each individual sensor signal can be easily identified, and their phase shifts measured.

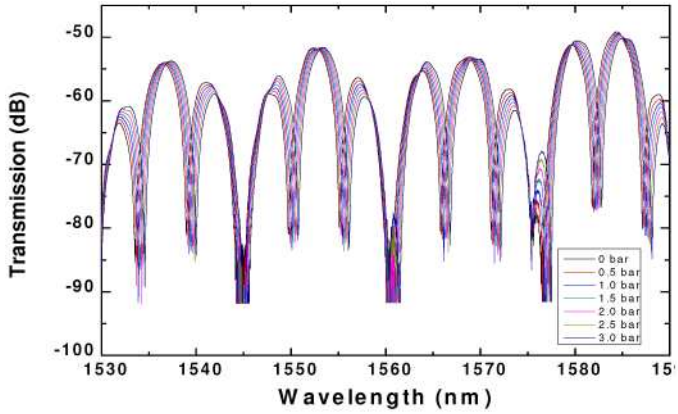

Fig. 5. Output transmission spectra of the two multiplexed Sagnac interferometric sensors in series with one sensor under applied pressure variations.

4.1 DWT Demultiplexing Method

The principle of the DWT demultiplexing method has been outlined in Ref [18]. When DWT is applied to a signal, it is decomposed and halved into high and low frequency components,

#115518 - $15.00 USD Received 10 Aug 2009; revised 20 Sep 2009; accepted 21 Sep 2009; published 29 Sep 2009

represented as detail and approximation coefficients, respectively. This is similar to applying both a high-pass and a low-pass filter simultaneously to a signal. Then, the approximation coefficients (i.e., low frequency components) of the signal can be further decomposed into 2nd-level detail and approximation coefficients. This iterative process continues until all individual sensor signals are separated and appear on different wavelet levels. In other words, it continues until the spatial frequency of the sensing signals matches with the frequency range at which the wavelet level represents. Figure 6 shows the extracted detail coefficients of the two sensors at different wavelet levels. By tracking their phase shifts, the response of the two sensors under various pressure levels can be detected. Figure 7(a) shows the phase shifts of the two sensors as a function of applied pressure. It is clear that PM-PCF2 shifted linearly with applied pressure, while PM-PCF1 remained about the zero shift position. The crosstalk between the two multiplexed sensor signals was also measured. The crosstalk given here is the ratio of the phase shift of PM-PCF1 (no pressure applied) to that of PM-PCF2 (pressured applied), and is shown in Fig. 7(b). It should be noted that, the crosstalk measurement represented here includes other sources of errors, such as measurement error and ambient noise. As can be seen from the figure, the crosstalk between the two sensors is less than 5% and decreases progressively at higher pressure values. This means the absolute crosstalk values are quite stable for the measured pressure range, and implies that the errors are mainly due to sources other than the actual crosstalk between the two sensors. On the other hand, if the crosstalk measurement shows a trend that correlates with the applied pressure, this would mean there is actual crosstalk present in the multiplexed sensor system.

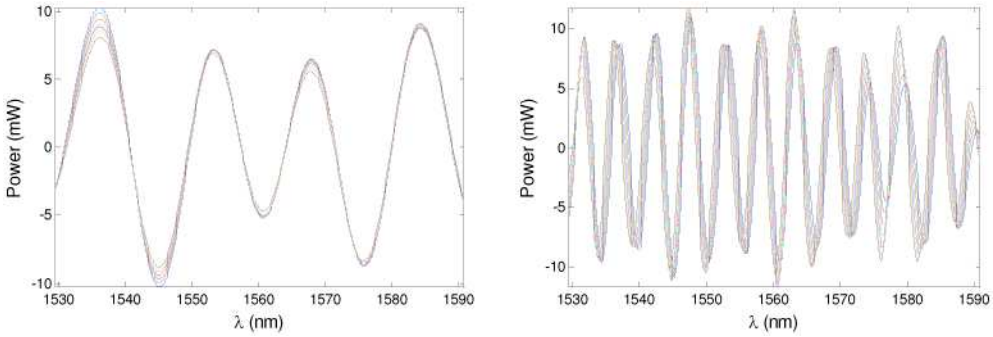

Fig. 6. Sensing signals of the two Sagnac interferometric sensors extracted using the wavelet method.

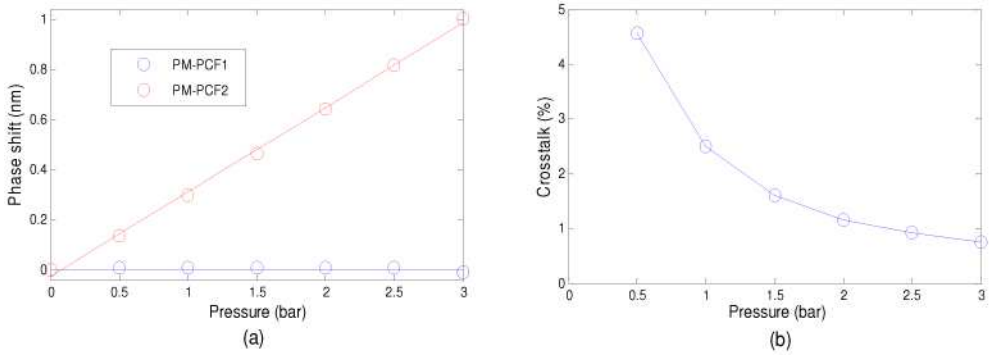

Fig. 7. (a) The wavelength shift as a function of pressure variation for the two Sagnac interferometric sensors, (b) sensing signal crosstalk of the two Sagnac interferometric sensors.

4.2 FT Demultiplexing Method

Besides the DWT, we also employed the FT method and the operating principle can be found in Ref [19]. The FT method works by transforming the multiplexed sensing signal from the

#115518 - $15.00 USD Received 10 Aug 2009; revised 20 Sep 2009; accepted 21 Sep 2009; published 29 Sep 2009

original (wavelength) domain, into its dual (spatial-frequency) domain, and is represented in the FT magnitude and phase spectra. Since the multiplexed signal is periodic, each individual sensor appeared as a finite amplitude peak in the FT magnitude spectrum; residing at a position dependent on the spatial frequency of the original sinusoidal signals. Thus, provided no two sensors have the same spatial frequency, each sensor can be distinctly identified. Normally, there are two ways of tracing the measurand-induced changes of individual sensors: (i) if the spatial-frequencies of the sensors change, measurands can be detected by the amount the amplitude peaks shift in the magnitude spectrum; and (ii) if the phase of the sensors change (and not the spatial-frequencies), measurands can be detected by the change of slope of the phase spectrum over the region corresponding to the amplitude peaks of the sensors in the magnitude spectrum. For the PM-PCF Sagnac interferometric sensors, when pressure was applied, the phase of the signals shifted proportionally while the spatial frequencies have no noticeable change, and so the second method applies. Figure 8 gives the FT magnitude and phase spectra of the multiplexed sensing signals after taking the FT. The corresponding regions of phase for the two sensors are shown in Fig. 9. From the figure, one can see that PM-PCF1 is held constant (no noticeable change in the phase slope), while PM-PCF2 is under a varying amount of applied pressure which resulted in a gradual change of the phase slope. The calculated equivalent wavelength shift and crosstalk between the two sensors are shown in Figs. 10(a) and 10(b), respectively. From the figure, the maximum crosstalk is ~5%, which is considered small.

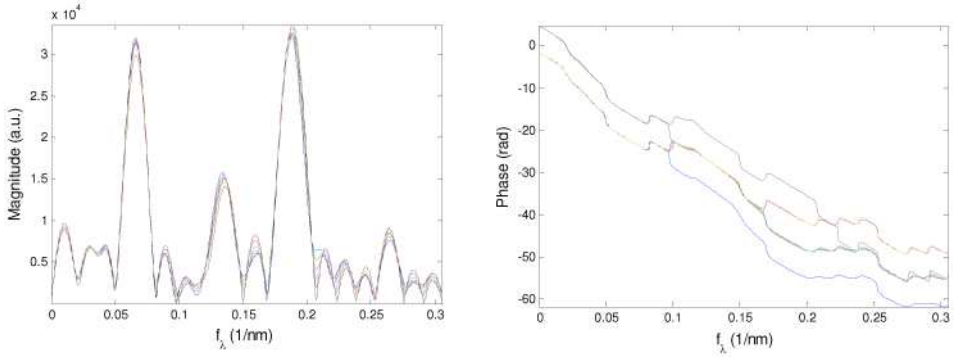

Fig. 8. Magnitude spectra and phase spectra of the sensing signal under Fourier transformation.

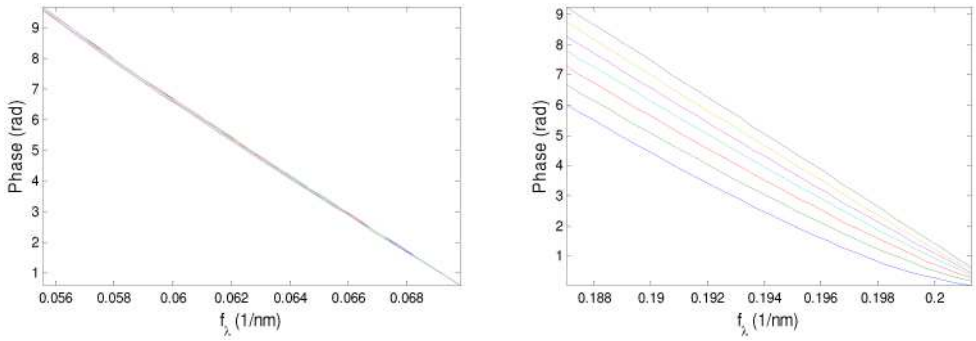

Fig. 9. Phase shift of the sensing signal from the two Sagnac interferometric sensors.

#115518 - $15.00 USD Received 10 Aug 2009; revised 20 Sep 2009; accepted 21 Sep 2009; published 29 Sep 2009

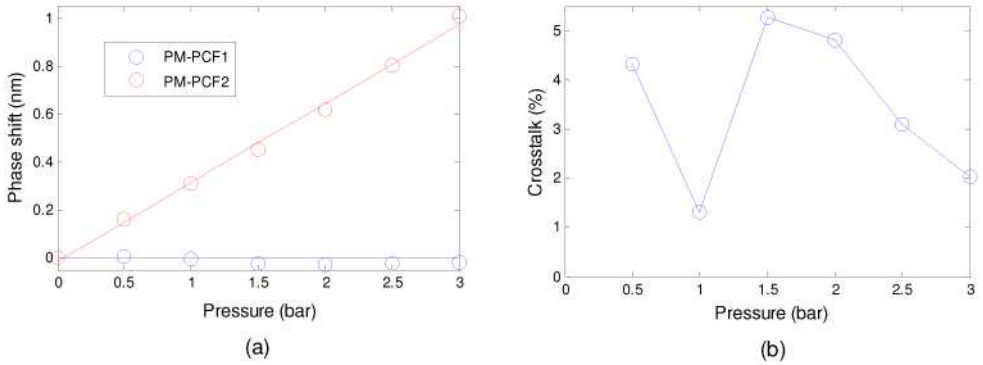

Fig. 10. (a) The wavelength shifts as a function of pressure variation for the two Sagnac interferometric sensors, (b) sensing signal crosstalk of the two Sagnac interferometric sensors.

5. Multiplexed in parallel by using coupler with reflected signals

The third multiplexing scheme is to multiplex Sagnac interferometric sensors in parallel, and is illustrated in Fig. 11. The effective lengths of PM-PCF1 and PM-PCF2 are 20 cm and 60 cm, respectively. The source light is split equally by the 3-dB coupler into two paths to illuminate the two sensors separately. The sensing signals reflected back from the two sensors are then coupled together by the same 3-dB coupler, and were measured with an OSA. The unused ends of the sensors were coiled in small loops to minimize Fresnel reflections. As compared to the serial multiplexing scheme, it required an additional 3-dB coupler. Note that the reflected sensing signals were taken instead of the transmitted signals, and there were two reasons for it. First, it helped to use one less 3-dB coupler to combine individual sensor signals at the output side and so reduced the system cost and complexity. Second, the reflected signal spectrum is, mathematically, the complement of the transmitted spectrum; and since the spectrum is of the form of sinusoidal pattern, the only difference is the phase angle of π. For K Sagnac interferometric sensors multiplexed in parallel, the output spectrum is given by,

$$\frac{P_{output}}{P_{input}} = 10Log_{10}\sum_{k=1}^{K}\left(\frac{1}{2}R_k L_k\left[1+\cos(\frac{2\pi}{S_k}+\theta_k)\right]\right)[\mathrm{dB}], \qquad (4)$$

where R_k, L_k, S_k, θ_k are the coupling ratio, the loss, the period of the output spectrum and the initial phase of the k-th sensor, respectively. Note that the output spectrum is the arithmetic sum of all individual sensor signals, as opposed to multiplication in the serial multiplexing case.

#115518 - $15.00 USD Received 10 Aug 2009; revised 20 Sep 2009; accepted 21 Sep 2009; published 29 Sep 2009

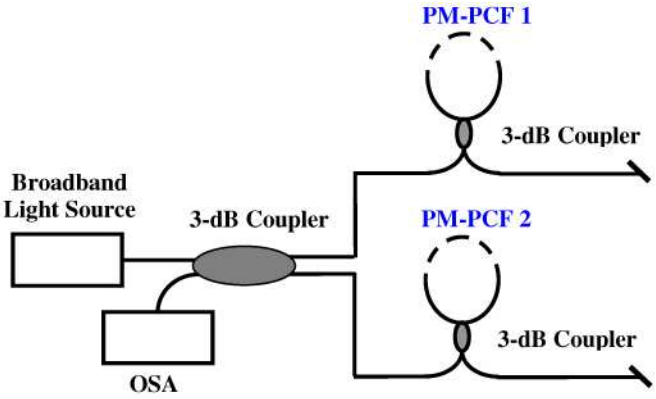

Fig. 11. Experimental setup of in parallel multiplexing technique for PM-PCF based Sagnac interferometric sensors.

As an experimental demonstration, a similar pressure sensing experiment to the previous multiplexing scheme was performed. Figure 12 shows the output spectra, with PM-PCF1 placed freely on the table and PM-PCF2 placed inside the pressure chamber. Again, we employed both the DWT and FT methods independently to demultiplex the sensing signal.

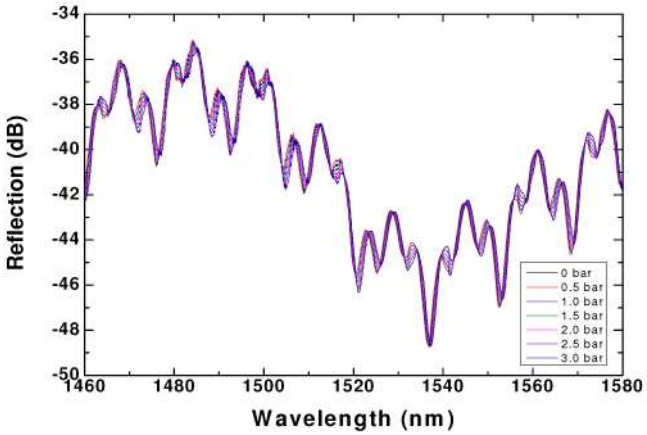

Fig. 12. Output transmission spectra of the two multiplexed Sagnac interferometric sensors in parallel with one sensor under applied pressure variations.

5.1 DWT Demultiplexing Method

After taking the DWT of the multiplexed sensing signal, Fig. 13 shows the detail coefficients of the two sensors at different wavelet levels. It is apparent from the figure that PM-PCF 1 remained almost constant, while PM-PCF2 can visibly be seen to have had the whole signal shifted. The phase shifts of the two sensors and the corresponding crosstalk measurement are shown in Figs. 14(a) and 14(b), respectively. The crosstalk between the two sensing signals is indeed very small, with a maximum value of less than 2%.

#115518 - $15.00 USD Received 10 Aug 2009; revised 20 Sep 2009; accepted 21 Sep 2009; published 29 Sep 2009

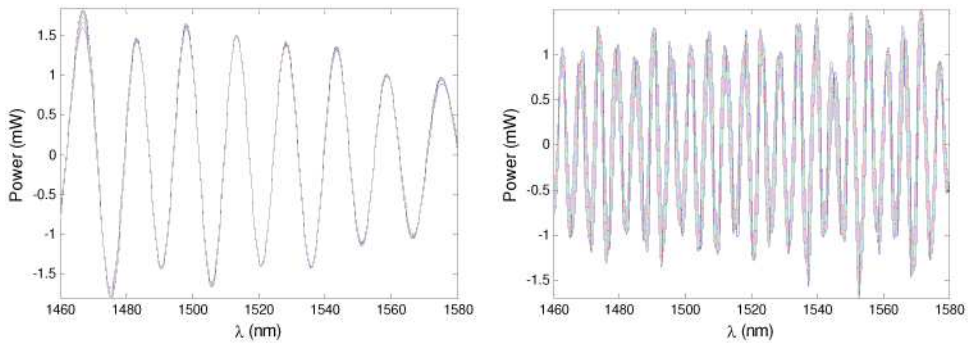

Fig. 13. Sensing signals of the two Sagnac interferometric sensors extracted using the wavelet method.

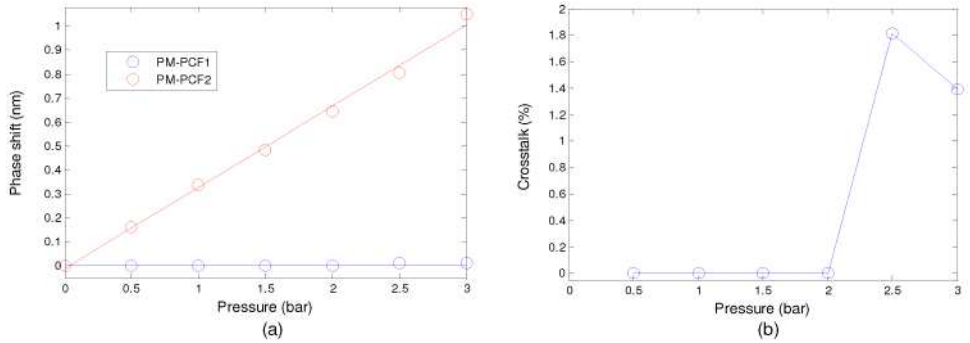

Fig. 14. (a) The wavelength shifts as a function of pressure variation for the two Sagnac interferometric sensors, (b) sensing signal crosstalk of the two Sagnac interferometric sensors.

5.2 FT Demultiplexing Method

With the FT method applied, Fig. 15 gives the FT magnitude and phase spectra of the multiplexed sensing signals. The corresponding regions of phase for the two sensors are illustrated in Fig. 16. From the figure, one can notice that PM-PCF1 has no noticeable change in the phase slope, while PM-PCF2 experienced pressure changes which resulted in a gradual change in the phase slope. The calculated equivalent wavelength shifts and the corresponding crosstalk measurement are shown in Figs. 17(a) and 17(b), respectively. Again, the crosstalk is very small, with a maximum of less than 3%.

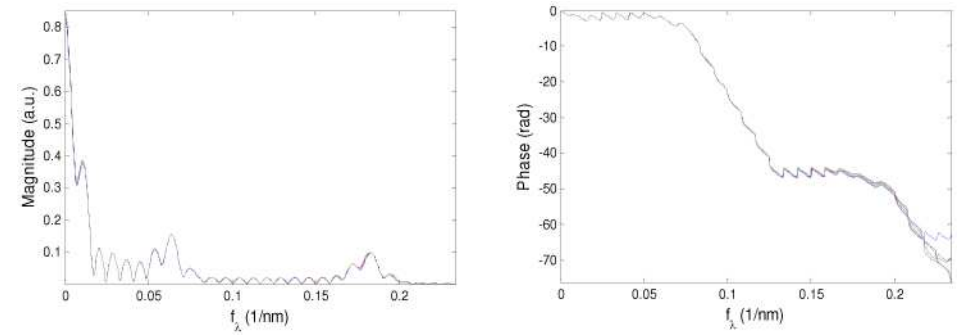

Fig. 15. Magnitude spectrum and phase spectrum of the sensing signal under Fourier transformation.

#115518 - $15.00 USD Received 10 Aug 2009; revised 20 Sep 2009; accepted 21 Sep 2009; published 29 Sep 2009

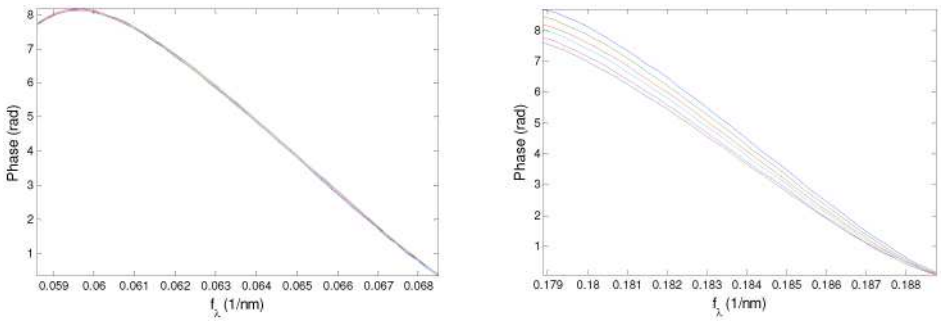

Fig. 16. Phase shift of the sensing signal from the two Sagnac interferometric sensors.

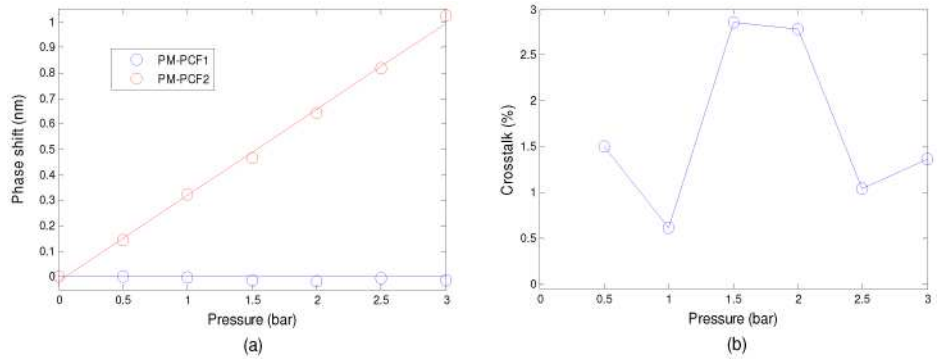

Fig. 17. (a) The wavelength shifts as a function of pressure variation for the two Sagnac interferometric sensors, (b) sensing signal crosstalk of the two Sagnac interferometric sensors.

6. Discussions

Each of the three multiplexing schemes has its own characteristics and is suitable for different applications. The CWDM scheme enables easy real-time system implementation. It provides a direct measurement without the need for dealing with crosstalk between signals from different channels. The number of sensors that can be multiplexed is limited by the available channels of the CWDM at a fixed light source bandwidth. Although with more channels, more sensors can be multiplexed; the bandwidth of each channel becomes narrower. In principle, the minimum bandwidth of each channel has to be larger than the period of the sensor signal, plus a bit of guard band between channel edges to avoid erroneous results due to signal discontinuities.

For the serial multiplexing scheme, no additional fiber-optic components are needed. The sensors are multiplexed easily by connecting them together one by one, which makes this scheme the simplest in terms of sensor system architecture. The number of sensors that can be multiplexed is mainly limited by the splicing loss between PM-PCFs and SMFs. On the other hand, for the parallel multiplexing scheme, it requires the addition of fiber couplers, which makes the system architecture relatively more complex and increases the total system cost. In addition, it increases the insertion loss due to splicing and fiber couplers. Nevertheless, the errors and adverse effects are also less because individual sensor signals are added rather than multiplied, and so they do not suffer from spectral shadowing and nonlinear mapping as is found in the serial multiplexing scheme [17]. It is evident from our experiments that parallel multiplexing has less crosstalk (with other sources of errors included) than that of serial multiplexing. It should be pointed out that the measurement errors due to fluctuations in the applied pressure played a role in our results, which can be noticed in their deviation from ideal values. This implies the intrinsic crosstalk is believed to be quite low.

#115518 - $15.00 USD Received 10 Aug 2009; revised 20 Sep 2009; accepted 21 Sep 2009; published 29 Sep 2009

There is a consideration when using the DWT and FT methods to demultiplex the sensor signals obtained from the serial and parallel multiplexing schemes. The effective length of PM-PCFs must be properly chosen not to be too close to each other in order to avoid overlap after performing the transformations. However, it is not an issue for the CWDM scheme because signals from sensors are well distinguished by each channel. These three multiplexing schemes can be implemented together to further increase the number of sensors. For example, within each channel in the CWDM, sensors can be multiplexed in series or in parallel. This combined configuration cannot only increase the number of sensors by several times, but also maximizes the full use of the light source bandwidth.

To sum up, from practicability point of view, the CWDM scheme is among the easiest and simplest, whereas serial multiplexing is more practical in real applications. On the other hand, parallel multiplexing offers slightly better performance in terms of crosstalk and measurement errors. At present stage, the main limitations on the last two multiplexing schemes are the insertion loss. The presented multiplexing schemes, together with the two demultiplexing methods, are not only limited to use for PM-PCF Sagnac interferometric sensors. Indeed, they can be applied in any PCF sensor that has sinusoidal patterns. This will be one step closer towards a more practical sensing system using PCF based sensors.

7. Conclusions

We have presented and experimentally demonstrated three different multiplexing schemes for PM-PCF based Sagnac interferometric sensors. The CWDM scheme is a simple and straightforward method in which we only need to measure the spectrum of each channel that corresponds to the sensor. Multiplexing of sensors in series along a single fiber has a simple architecture, whereas multiplexing in parallel is slightly more complex and requires more fiber-optic components as the number of sensors get larger. The latter two multiplexing schemes have complex measured spectra that cannot be easily demultiplexed. Two demultiplexing methods based on the DWT and FT have been successfully applied to the multiplexed sensing signals, and both yielded good results with small crosstalk. The three multiplexing schemes and the two demultiplexing methods can be applied to any PCF sensor that has sinusoidal patterns, which makes them a general purpose technique for PCF based sensor systems.

Acknowledgments

The funding support of this work in part by the University Grants Council's Matching Grant of the Hong Kong Special Administrative Region Government under the Niche Areas project J-BB9J and in part by the Hong Kong Polytechnic University Central Research Grant (grant no.: G-YX2C), are gratefully acknowledged. H. Y. Fu and A. C. L. Wong contributed equally in this work

#115518 - $15.00 USD Received 10 Aug 2009; revised 20 Sep 2009; accepted 21 Sep 2009; published 29 Sep 2009